

- Browning KA, Roberts NM.** 1994. Structure of a frontal cyclone. *Q. J. R. Meteorol. Soc.* **120**: 1535–1557.
- Carlson TN.** 1980. Airflow through midlatitude cyclones and the comma cloud pattern. *Mon. Weather Rev.* **108**: 1498–1509.
- Collins English Dictionary.** 2005. Definition of saddle point [accessed 14 March 2022. Most material © 2005, 1997, 1991 by Penguin Random House LLC. Modified entries © 2019 by Penguin Random House LLC and HarperCollins Publishers Ltd. Word origin [1920–25]].
- Dacre HF, Clark PA, Martínez-Alvarado O et al.** 2015. How do atmospheric rivers form? *Bull. Am. Meteorol. Soc.* **96**: 1243–1255.
- Dacre HF, Martínez-Alvarado O, Mbengue CO.** 2019. Linking atmospheric rivers and warm conveyor belt airflows. *J. Hydrometeorol.* **20**: 1183–1196.
- Drazin PG.** 1992. Nonlinear systems. In: *Cambridge Texts in Applied Mathematics*. Cambridge University Press: Cambridge, UK.
- Gentile ES, Gray SL, Barlow JF et al.** 2021. The impact of atmosphere–ocean–wave coupling on the near-surface wind speed in forecasts of extratropical cyclones. *Bound. Layer Meteorol.* **180**: 105–129.
- Gimeno L, Nieto R, Vázquez M et al.** 2014. Atmospheric rivers: a mini-review. *Front. Earth Sci.* **2**: 2.
- Hart NC, Gray SL, Clark PA.** 2015. Detection of coherent airstreams using cluster analysis: application to an extratropical cyclone. *Mon. Weather Rev.* **143**: 3518–3531.
- Hersbach H, Bell B, Berrisford P et al.** 2020. The ERA5 global reanalysis. *Q. J. R. Meteorol. Soc.* **146**: 1999–2049.
- Hodges KI.** 1995. Feature tracking on the unit sphere. *Mon. Weather Rev.* **123**: 3458–3465.
- Lavers DA, Allan RP, Wood EF et al.** 2011. Winter floods in Britain are connected to atmospheric rivers. *Geophys. Res. Lett.* **38**: 1–8.
- Lavers DA, Villarini G, Allan RP et al.** 2012. The detection of atmospheric rivers in atmospheric reanalyses and their links to British winter floods and the large-scale climatic circulation. *J. Geophys. Res. Atmos.* **117**: D20106. <https://doi.org/10.1029/2012JD018027>
- Met Office.** 2018. Strong winds and heavy rain from storms ali and bronagh. <https://www.metoffice.gov.uk/binaries/content/assets/metofficegovuk/pdf/weather/learn-about/uk-past-events/interesting/2018/strong-winds-and-heavy-rain-from-storms-ali-and-bronagh---met-office.pdf> [accessed 25 November 2021].
- Najman L, Schmitt M.** 1994. Watershed of a continuous function. *Signal Process.* **38**: 99–112.
- Newell RE, Newell NE, Zhu Y et al.** 1992. Tropospheric rivers? A pilot study. *Geophys. Res. Lett.* **19**: 2401–2404.
- Papritz L, Aemisegger F, Wernli H.** 2021. Sources and transport pathways of precipitating waters in cold-season deep north Atlantic cyclones. *J. Atmos. Sci.* **78**: 3349–3368.
- Pérez-Muñuzuri V, Eiras-Barca J, Garaboa-Paz D.** 2018. Tagging moisture sources with Lagrangian and inertial tracers: application to intense atmospheric river events. *Earth Syst. Dyn.* **9**: 785–795.
- Pfahl S, Wernli H.** 2012. Quantifying the relevance of cyclones for precipitation extremes. *J. Clim.* **25**: 6770–6780.
- Ralph FM, Dettinger MD, Cairns MM et al.** 2018. Defining “atmospheric river”: how the Glossary of Meteorology helped resolve a debate. *Bull. Am. Meteorol. Soc.* **99**: 837–839.
- Shields CA, Rutz JJ, Leung L-Y et al.** 2018. Atmospheric river tracking method intercomparison project (ARTMIP): project goals and experimental design. *Geosci. Model Dev.* **11**: 2455–2474.
- Sodemann H, Wernli H, Knippertz P et al.** 2020. *Structure, Process, and Mechanism*. Springer: New York, NY, pp 15–43.
- Wernli H.** 1997. A Lagrangian-based analysis of extratropical cyclones. II: a detailed case-study. *Q. J. R. Meteorol. Soc.* **123**: 1677–1706.
- Wernli H, Davies H.** 1997. A Lagrangian-based analysis of extratropical cyclones. I: the method and some applications. *Q. J. R. Meteorol. Soc.* **123**: 467–489.
- Young MV, Monk GA, Browning KA.** 1987. Interpretation of satellite imagery of a rapidly deepening cyclone. *Q. J. R. Meteorol. Soc.* **113**: 1089–1115.

Correspondence to: S. Cuckow




s.cuckow@pgr.reading.ac.uk

© 2022 The Authors. Weather published by John Wiley & Sons Ltd on behalf of the Royal Meteorological Society

This is an open access article under the terms of the Creative Commons Attribution License, which permits use, distribution and reproduction in any medium, provided the original work is properly cited.

doi: 10.1002/wea.4212

North Atlantic Oscillation response to the Madden–Julian Oscillation in a coupled climate model

Daniel T. Skinner¹ ,
Adrian J. Matthews^{1,2} ,
and David P. Stevens¹ 

¹Centre for Ocean and Atmospheric Sciences, School of Mathematics, University of East Anglia, Norwich, UK

²Centre for Ocean and Atmospheric Sciences, School of Environmental Sciences, University of East Anglia, Norwich, UK

Introduction

The Madden–Julian Oscillation (MJO; Madden and Julian, 1971) is the leading

mode of intra-seasonal variability in the tropics and is characterised by an area of enhanced deep convection, which travels eastward across the Maritime Continent with a period of 30–60 days. This area of enhanced convection is associated with divergence in the upper troposphere and is followed directly by an area of suppressed convection associated with convergence in the upper troposphere.

This divergent circulation produced by latent heat release in the MJO's enhanced convective phase excites Rossby waves, which interact with various extratropical weather regimes to create so-called teleconnection patterns. Through these teleconnections, the weather experienced around

the globe can be linked back to the weather in the tropics.

The North Atlantic Oscillation (NAO; Walker and Bliss, 1932) is a key mode of winter variability in northern Europe. Thus, understanding the behaviour of the NAO is key to accurate United Kingdom (UK) weather prediction. The NAO is characterised by a positive and a negative phase, which bring different types of weather to the UK. During the winter, the NAO+ is associated with warmer, stormier weather, while the reverse relationship is observed for the NAO–.

Through observational studies, the NAO is known to be forced at least in part by the MJO (Cassou, 2008; Lin et al., 2010). In this

article, we will assess the fidelity of these teleconnections in the latest global coupled model from the UK Met Office.

The HadGEM3-GC3.1 model

We analyse the Met Office Hadley Centre Global Environment Model in the Global Coupled configuration 3.1 with a medium resolution atmosphere and ocean (HadGEM3-GC3.1-MM). For a full description of the model and historical experiment, see Williams *et al.* (2018) and Andrews *et al.* (2020), respectively. This model formed part of the sixth phase of the Coupled Model Intercomparison Project (CMIP6) – a collaboration between climate modelling centres from around the globe with the goal of standardising coupled model experiments. In particular, we will focus on the ‘historical’ experiment runs, which used the CMIP6 defined forcings. This allows for an assessment of MJO–NAO teleconnections in contemporary climate conditions. The historical experiment runs from 1850 to 2014 (inclusive), but we will focus on the final 30 years of this period (1985–2014) to align with the availability of high-quality reanalysis data.

Methodology

In order to analyse the MJO and its effects, we use the index created by Wheeler and Hendon (2004). This index is constructed from daily mean values of outgoing longwave radiation (OLR) and zonal wind at the 200 and 850hPa pressure levels (U200 and U850, respectively). Due to the availability of model wind data in CMIP6, we will use 250hPa zonal wind (U250) instead of U200, although analysis has shown that this has little qualitative effect on the outcomes. On each day, the index assigns a value for the MJO amplitude and phase. The amplitude is a positive number which describes the strength of the anomalous convection. On days when the amplitude is greater than one, the MJO is said to be active and this day will be included in our analysis. The phase takes an integer value between one and eight and describes the longitudinal location of the convective centres. Figure 1 shows boreal winter (November–April) composites of OLR (which is used as an analogue for convection) in each of the eight phases. For example, phase 1 (Figure 1a) represents enhanced convection over the western Indian Ocean and phase 8 (Figure 1h) represents enhanced convection over the mid to eastern Pacific Ocean.

The NAO can be characterised by the difference in anomalous pressure between Iceland and the Azores. Therefore, we define our index as the normalised difference between two area averages of 500hPa geopotential

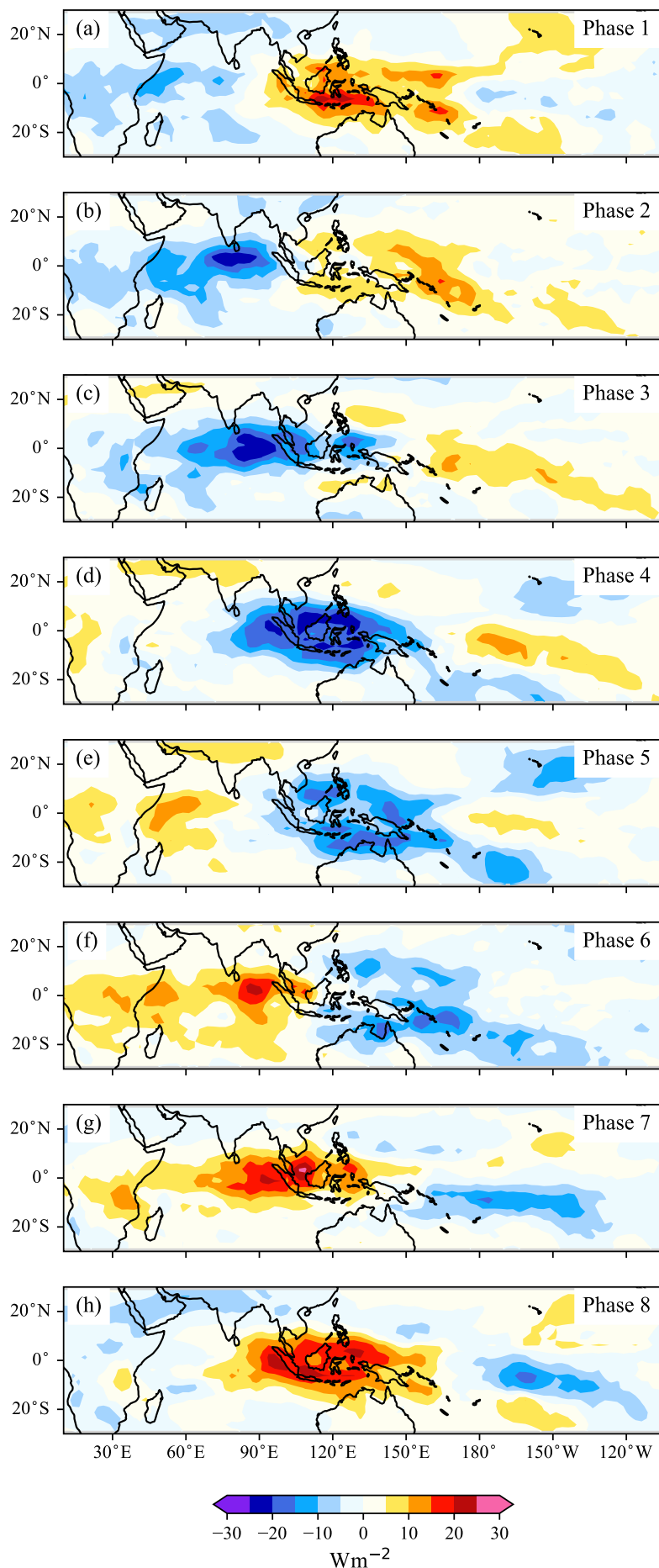


Figure 1. Boreal winter Madden–Julian Oscillation phase composites of outgoing longwave radiation (OLR) anomaly over the period 1985–2014 in HadGEM3-GC3.1-MM. Here, a negative anomaly in OLR is analogous to increased anomalous convection.

height (Z500) anomaly.¹ The two areas are chosen to suitably encompass the centres of the pressure variation (50–70°N, 10–50°W and 30–45°N, 5–55°W). This method of calculating the NAO index is similar to that of Cropper *et al.* (2015). However, we average the geopotential height anomaly over a larger area to account for the fact that the centres of action can be shifted in models. Our index is a time series, in which each day is either defined to be 'NAO+', 'NAO–' or 'inactive' depending on whether the index exceeds one standard deviation in magnitude and whether its sign is positive or negative. As for the MJO, we can create boreal winter composites to visualise the positive and negative NAO regimes (Figure 2). Note that this index is slightly different to that used by Cassou (2008) as we are focussing solely on the NAO.

With time series for both the MJO phase and the state of the NAO, the link between the two may then be analysed. Following Cassou (2008), we calculate the frequency of days in which an NAO state is active for each MJO phase in turn. We then obtain a percentage change in the probability of observing each state from the climatological mean probability when a given MJO phase is active. This is then repeated with a lag (MJO leading) of 1–20 days to ascertain how the NAO responds in the days and weeks following each MJO phase.

To test for statistical significance in the frequency of an NAO state's occurrence, we employ a Student's *t*-test at the 95% confidence level. The population dataset is taken to be the value of the normalised NAO index over the whole time domain, while the sample dataset consists of only the days that fall within the given MJO phase (with some given lag). The relative frequency of each NAO state is then compared between the population and sample. This is equivalent to the second of the two significance tests used by Cassou (2008). We have not used the first significance test from Cassou (2008) due to differences in methodology, as we do not assign every day in our analysis to either NAO+ or NAO–.

The model is compared with observed/reanalysis data taken from the ERA-Interim reanalysis product (U250, U850 and Z500) and the NOAA-interpolated OLR dataset. Hereafter, this will be referred to simply as the observational data. The above analysis is applied to both the model and observational data so that differences between the two may be assessed.

Results

The results of our analysis into the NAO response to each MJO phase for both the

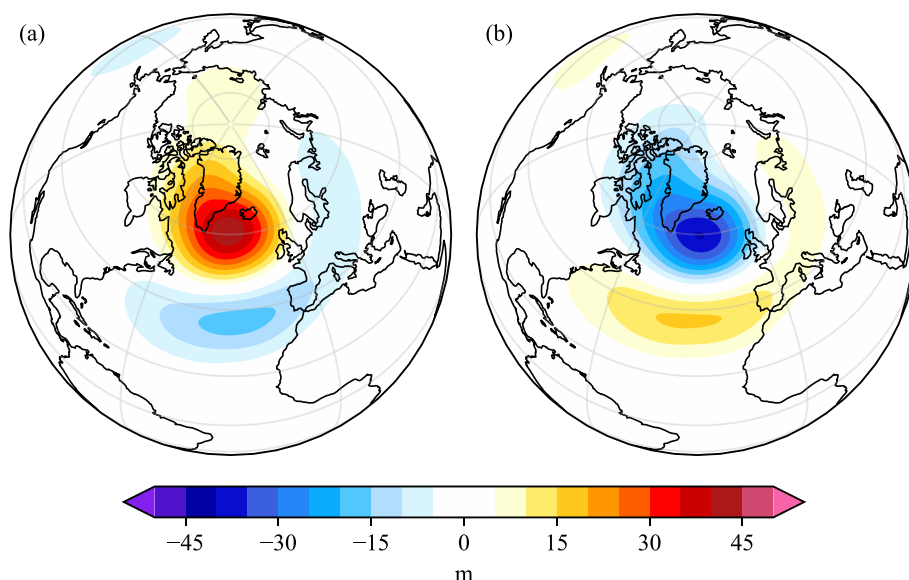


Figure 2. Boreal winter (a) negative North Atlantic Oscillation (NAO–) and (b) NAO+ Z500 anomaly composites over the period 1985–2014 in HadGEM3-GC3.1-MM.

model and observational data are presented in Figure 3. We note that both the magnitude and rate of change of the response are of interest, as the magnitude indicates the strength of the NAO response, while a steep gradient indicates a more direct link between the given MJO phase and NAO state. There are strong responses (over 30% change in probability of observing either NAO+ or NAO–) to a number of MJO phases in the model, which are statistically significant compared to the climatological mean. In general, the NAO response to the MJO in the HadGEM3-GC3.1-MM model is often of the same sign as the NAO response to the MJO in the observations (Figure 3). The model replicates the observed response particularly well in a small number of cases (phases 1 and 8).

However, there are other MJO phases in which the NAO response is either suppressed or even of the wrong sign, particularly at lags of more than one week. Two key teleconnection patterns identified by Cassou (2008), which are visible in the observational data, are the responses of NAO+ and NAO– to MJO phases 3 and 6, respectively. Both of these teleconnections act as useful predictors for the NAO state and so are the focus of our investigation.

In the observational data, the lag 0 NAO+ response to MJO phase 3 is zero (i.e. climatological probability of observing NAO+). After approximately one week, the probability of occurrence of NAO+ rises by more than 30%, implying predictability of entering an NAO+ regime. However, in the model, the chances of experiencing an NAO+ event are approximately constant from lag 0 onwards, at 20% higher than the climatological mean. It is encouraging that the model at least predicts the correct sign for the response; however, the time dependence of this link

is not well reproduced by the HadGEM3 model or the CMIP6 model mean.

There is a strong NAO– response to MJO phase 6 in the observational data. In this case, the response peaks approximately two weeks after phase 6 and exhibits a 47% increase in NAO– occurrence, suggesting phase 6 as a precursor to an NAO– event. The model replicates the response well for approximately one week. However, at longer lags, it shows a statistically significant decrease in the probability of NAO–. The reasons for the difference should be explored further.

In the observational results we see that, for the most part, the NAO response to one MJO phase approximately follows on from the response to the preceding phase, but lagged by 5–10 days. This indicates that the eight MJO phases are occurring in a sequential manner as we would expect. For example, in MJO phase 4, the NAO+ response peaks at lag 3 days, while in phase 3, it peaks at lag 8 days. In the model, this is not the case, as we see no significant NAO+ response to MJO phase 4. The relationship between these two phases seems to be much weaker, indicating that the model MJO may not be behaving as observed.

MJO events spend less time in each phase in the model than in observations (Figure S2a), so we may infer that the MJO propagation is faster in the model. The timescales over which the MJO propagates are very similar to the timescales over which the extratropics responds to the MJO (that is, the time that the MJO spends in each phase is similar to the lag between changes in the MJO and NAO). Therefore, a change to the propagation speed of the MJO means that the NAO response to a given phase will occur within a different atmospheric state. Both Yadav and Straus (2017) and

¹We show that the results obtained using Z500 are similar to those obtained when using mean sea-level pressure in Figure S1 in the Supporting Information.

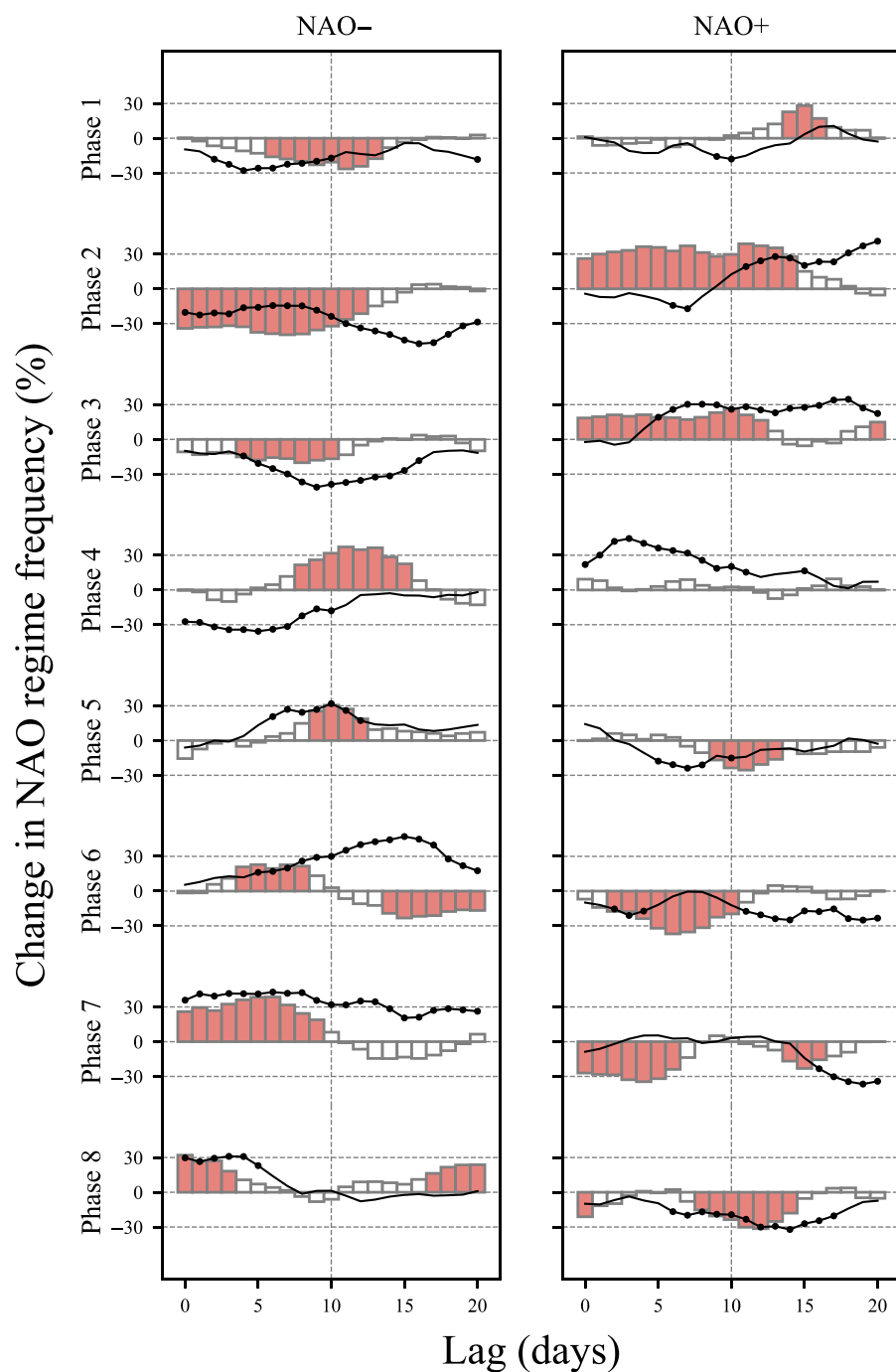


Figure 3. North Atlantic Oscillation (NAO) response to the Madden-Julian Oscillation (MJO). The bars represent the percentage change in the probability of observing a particular NAO state, at a given lag after observing a particular MJO phase, in the HadGEM3-GC3.1-MM model. Bars that are coloured in red represent a change that is statistically significant at the 95% level. The NAO response to the MJO in the observed data is plotted as the black line, with circular markers to indicate significance.

Yadav *et al.* (2019) have shown that these changes in MJO propagation speed can alter the NAO response to the MJO. It is likely that this is one reason why some of the sequential manner of the NAO response is lost. Interestingly, the total number of days spent in each MJO phase is similar between the model and observations, suggesting that although the MJO is propagating faster, there are also more individual events (Figure S2c).

Among other reasons for this seeming lack of continuity is a stalling or dissipation of

the MJO as it propagates over the Maritime Continent. Ahn *et al.* (2020) showed that the HadGEM3-GC3.1-MM model performs well compared to other CMIP6 models in capturing the MJO propagation over the Maritime Continent, and this has been backed up by our own investigations. We have shown that although the MJO is propagating faster in the model than observations, this difference is approximately the same across all eight MJO phases rather than being confined to those phases in which the MJO is passing over the Maritime Continent. This

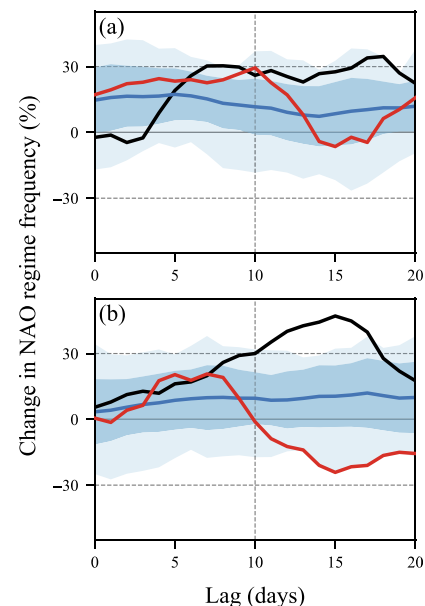


Figure 4. (a) North Atlantic Oscillation (NAO+) response to Madden-Julian Oscillation (MJO) phase 3 and (b) NAO- response to MJO phase 6. The blue line represents the multi-model mean from 25 CMIP6 coupled climate models, with a band of ± 1 standard deviation given by the dark blue shading and the multi-model range given by the light blue shaded region. The HadGEM3-GC3.1-MM individual model response is shown by the red line and the observed response is shown by the black line.

should be considered when analysing other models.

Discussion

We have shown that HadGEM3-GC3.1-MM exhibits a significant NAO response to the MJO, but that this response is not necessarily in line with that seen in observations, including NAO responses in some phases which are too weak or the wrong sign. We may, therefore, question the model's ability to predict the NAO at lead times of more than one week when tropical-extratropical interactions become important, whilst being mindful of the fact that the MJO is only one of many sources of tropical teleconnections to the North Atlantic (Scaife *et al.*, 2017). The results presented above pertain to just one model. However, by analysing an ensemble of models from the CMIP6 project, we may hope to find a more accurate representation of the NAO response to the MJO.

Figure 4 shows the two key teleconnections (NAO+ response to MJO phase 3 and NAO- response to MJO phase 6) discussed above for the observational and HadGEM3-GC3.1-MM datasets alongside a summary of 25 CMIP6 models (see Table S1 for a full list). We find that the majority of the models, including HadGEM3-GC3.1-MM, significantly underestimate the magnitude of the response of the NAO. Even the most extreme response from the models (shown

by the light blue shading in Figure 4b) cannot simulate the large observed response in NAO– to MJO phase 6. This is in agreement with previous works that have highlighted weakened teleconnections in climate models (Vitart, 2017; Scaife and Smith, 2018).

A considerable number of the models predict the opposite sign for the response, suggesting confounding errors in the modelling of the processes behind the teleconnection patterns. One candidate for this is bias in the representation of the climatological mean state. In particular, errors in the representation of the strength and position of the jet streams will lead to errors in the propagation of the wave trains, which underpin the teleconnection patterns (Dawson *et al.*, 2011).

To accurately simulate MJO–NAO teleconnection patterns, models must first have accurate representations of the MJO, the climatological mean state (Henderson *et al.*, 2017), wave trains, the stratospheric polar vortex (Barnes *et al.*, 2019) and the NAO. The complexity of these processes and linkages between them make the MJO–NAO teleconnection problem challenging to model. Even though the HadGEM3-GC3.1-MM model performs well among CMIP6 models in simulating the MJO propagation over the Maritime Continent (Ahn *et al.*, 2020), this is countered by the excessive speed of the MJO propagation. Hence, it is still unable to simulate the full range of processes needed to accurately model MJO–NAO teleconnections.

Further questions

The results obtained in this study open a number of opportunities for further investigation. The methodology described above has been designed to translate efficiently between different datasets, meaning that this work can be extended to a number of different questions. Also, the framework used is not specific to the NAO, so other MJO teleconnections (for example, to the Pacific–North American pattern) may be considered in a similar way.

A natural progression of this study would include a deeper look at some of the other CMIP6 models, including some consideration of large ensemble experiments implemented by some modelling centres. Another avenue for investigation is the temporal variability of MJO–NAO interactions. We have

presented results for a single time frame, but recent works (e.g. Lee *et al.*, 2019) have shown that these teleconnections can be modulated by seasonal to decadal variations, such as the El Niño–Southern Oscillation.

Acknowledgements

The research presented in this paper was carried out on the High Performance Computing Cluster supported by the Research and Specialist Computing Support service at the University of East Anglia and on JASMIN, the UK's collaborative data analysis environment. All CMIP6 data were accessed from the CEDA archive – more details are provided in Table S1. We thank the two independent reviewers for their constructive feedback, which helped to improve and clarify this manuscript.

References

- Ahn M-S, Kim D, Kang D *et al.* 2020. MJO propagation across the maritime continent: are CMIP6 models better than CMIP5 models? *Geophys. Res. Lett.* **47**(11): e2020GL087250.
- Andrews MB, Ridley JK, Wood RA *et al.* 2020. Historical simulations with HadGEM3-GC3.1 for CMIP6. *J. Adv. Model. Earth Syst.* **12**(6): e2019MS001995.
- Barnes EA, Samarasinghe SM, Ebert-Uphoff I *et al.* 2019. Tropospheric and stratospheric causal pathways between the MJO and NAO. *J. Geophys. Res. Atmos.* **124**: 9356–9371.
- Cassou C. 2008. Intraseasonal interaction between the Madden–Julian Oscillation and the North Atlantic Oscillation. *Nature* **455**(7212): 523–527.
- Cropper TE, Hanna E, Valente MA *et al.* 2015. A daily Azores–Iceland North Atlantic Oscillation index back to 1850. *Geosci. Data J.* **2**(1): 12–24.
- Dawson A, Matthews AJ, Stevens DP. 2011. Rossby wave dynamics of the North Pacific extra-tropical response to El Niño: importance of the basic state in coupled GCMs. *Clim. Dyn.* **37**: 391–405.
- Henderson SA, Maloney ED, Son S-W. 2017. Madden–Julian Oscillation Pacific teleconnections: the impact of the basic state and MJO representation in general circulation models. *J. Clim.* **30**(12): 4567–4587.
- Lee RW, Woolnough SJ, Charlton-Perez AJ *et al.* 2019. ENSO modulation of MJO teleconnections to the North Atlantic and Europe. *Geophys. Res. Lett.* **46**: 13535–13545.
- Lin H, Brunet G, Fontecilla JS. 2010. Impact of the Madden–Julian Oscillation on the intraseasonal forecast skill of the North Atlantic Oscillation. *Geophys. Res. Lett.* **37**: L19803. <https://doi.org/10.1029/2010GL044315>
- Madden RA, Julian PR. 1971. Detection of a 40–50 day oscillation in the zonal wind in the tropical Pacific. *J. Atmos. Sci.* **28**(5): 702–708.
- Scaife AA, Comer RE, Dunstone NJ *et al.* 2017. Tropical rainfall, Rossby waves and regional winter climate predictions. *Q. J. R. Meteorol. Soc.* **143**: 1–11.
- Scaife AA, Smith D. 2018. A signal-to-noise paradox in climate science. *npj Clim. Atmos. Sci.* **1**: 28.
- Vitart F. 2017. Madden–Julian Oscillation prediction and teleconnections in the S2S database. *Q. J. R. Meteorol. Soc.* **143**: 2210–2220.
- Walker GT, Bliss EW. 1932. World Weather V. *Mem. R. Meteorol. Soc.* **4**(36): 53–84.
- Wheeler MC, Hendon HH. 2004. An all-season real-time multivariate MJO index: development of an index for monitoring and prediction. *Mon. Weather Rev.* **132**(8): 1917–1932.
- Williams KD, Copsey D, Blockley EW *et al.* 2018. The Met Office global coupled model 3.0 and 3.1 (GC3.0 and GC3.1) configurations. *J. Adv. Model. Earth Syst.* **10**(2): 357–380.
- Yadav P, Straus D. 2017. Circulation response to fast and slow MJO episodes. *Mon. Weather Rev.* **145**(5): 1577–1596.
- Yadav P, Straus D, Swenson E. 2019. The Euro–Atlantic circulation response to the Madden–Julian Oscillation cycle of tropical heating: coupled GCM intervention experiments. *Atmosphere–Ocean* **57**(3): 161–181.

Correspondence to: D. T. Skinner
d.skinner@uea.ac.uk

© 2022 The Authors. Weather published by John Wiley & Sons Ltd on behalf of Royal Meteorological Society.

This is an open access article under the terms of the Creative Commons Attribution License, which permits use, distribution and reproduction in any medium, provided the original work is properly cited.

doi: 10.1002/wea.4215

Supporting Information

Figures S1, S2, Table S1 and References.